OPTIMAL SMOOTHING FILTER CONFIGURATION FOR LOCAL GNSS AUGMENTATION IN CHALLENGING URBAN ENVIRONMENTS

5-7 December 2018
ESA/ESTEC, Noordwijk, The Netherlands

Daniel Gerbeth [(1)], **Maria Caamano** [(1)], **Mihaela-Simona Circiu** [(1)], **Michael Felux** [(1)]

[(1)] ***German Aerospace Centre (DLR)***
Linder Höhe
51147 Köln
Germany
Email: daniel.gerbeth@dlr.de

INTRODUCTION

The UAV (Unmanned Aerial Vehicle) field is a vastly growing market in recent years. Advances in technology in terms of batteries and miniaturized systems enable drone applications in more and more fields. Heavy interest is shown in fields like parcel delivery, surveillance or civil protection. Many of these applications potentially take place in challenging (in terms of navigation) urban environments.
When these applications are to be carried out in an autonomous way, having drones automatically flying missions and fulfilling tasks, a safe and reliable navigation is one key aspect. Only if a central control facility or a collaborative network is aware of the precise drone locations, operations can be carried out in a safe way.

When comparing the context of such urban drone operations to related fields like civil aviation, where safe and reliable satellite navigation is pursued already for decades, two major differences can be identified. One is the use of significantly different equipment, typically orders of magnitude cheaper than highest grade hardware in civil aviation but also designed for minimal weight and power consumption to meet the limitations in small UAV (few kg). These sensors are, as expected from such figures, typically also drastically less accurate and reliable. To compensate for this, more effort has to be put into integrating many data sources and compensating the weaknesses of the different systems as much as possible in a fused navigation system.
The second difference concerns the area of operation. While most of the flight time a civil aircraft is in open, controlled airspace the targeted operations for UAV in an urban context are mostly within lower airspace (< 500 ft.) with potentially strongly degraded signal reception of GNSS (Global Navigation Satellite System) signals, multipath, interferences and other threads to navigation (see Fig. 1).

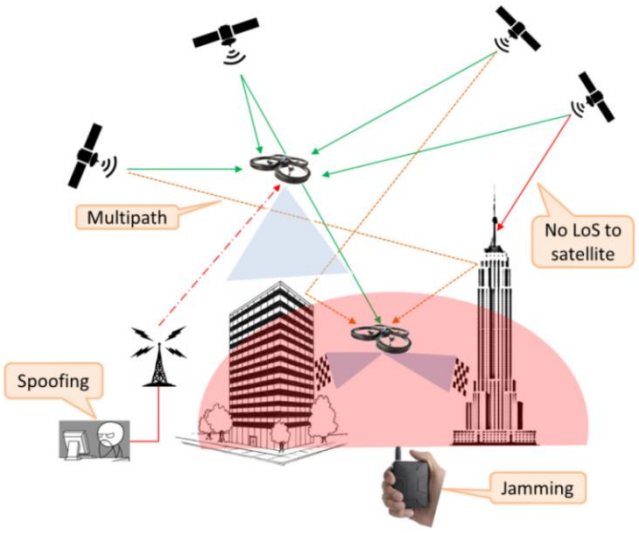

Fig. 1. Potential challenges for navigation in urban environments.

One means of tackling the challenges such an environment poses on navigation is the use of local GNSS augmentation. Reference stations in the area of operation, in a city scenario for example a few stations distributed over the urban area, continuously measure the GNSS signals. Knowing the exact location of these references allows the computation of corrections for the satellites signals. Additionally, this ground network can perform monitoring tasks, ensuring the signals are safe to be used by UAVs in the area. Range corrections and integrity information are then broadcast to users in the serviced areas.
Thereby locally corrected GNSS ranges can then be used for stand-alone navigation as in GBAS (Ground Based Augmentation System) or SBAS (Space Based Augmentation System) ([1] [2] [3] [4]), or even better, included into a multi-sensor-fusion navigation system for even more robust positioning [5]. Before using them for positioning the satellite pseudoranges are typically smoothed using carrier phase measurements by Hatch filtering [6]. Depending on the smoothing filter constant the residual noise levels converge towards the carrier phase noise which is in mm level compared to the code noise in the range of meters.

Here we find the trade-off that we want to study in this paper. While longer smoothing reduces the residual noise and therefore improves the positioning, it also means that satellites have to be continuously visible for a longer period (the filter convergence time) until they can be first used. In an environment where signals are regularly blocked by e.g. buildings around, this can significantly reduce the number of usable satellites at a given point, thus degrading the performance. For 5 different scenarios in two urban environments we perform simulations in terms of satellite visibility for various smoothing time constants to assess the resulting navigation performance along 20 minutes of drone trajectory.

SIMULATION SETUP

In this section a step by step description is given, how the performance simulations constituting the core part of this paper are performed. Based on models in terms of satellite orbits for different constellations (almanac data from GPS, Galileo and GLONASS), residual noise and multipath models from previous studies (see [7]) complemented with own measurements as well as 3D city models, we simulate satellite visibility and geometry for different trajectories trough urban and suburban scenarios.

3D City Models

The core simulations in this paper base on the use of 3D models from Berlin. The decision to perform these first simulations with 3D data from Berlin was mainly due to the availability of detailed models. These models are freely available for use through an online download portal [8]. Such data becomes available for more and more cities and even whole regions in the last years, making specific simulations and analysis as performed in this study potentially possible everywhere.
An example of the data used for simulation is given in Fig. 2. Even though exact figures in terms of accuracy of the models could not be found, at least meter-level precision is assumed. Apart from that, as this paper is mainly interested in relative variations that base on the average height and density of buildings as well as width of streets, a perfect mapping of the specific city is not required.
The 3D data is provided by the service in different formats including CityGML (considered the standard for 3D description of cities and landscapes [9]) and *.3ds*, a proprietary format. As the Unity framework [10] was used

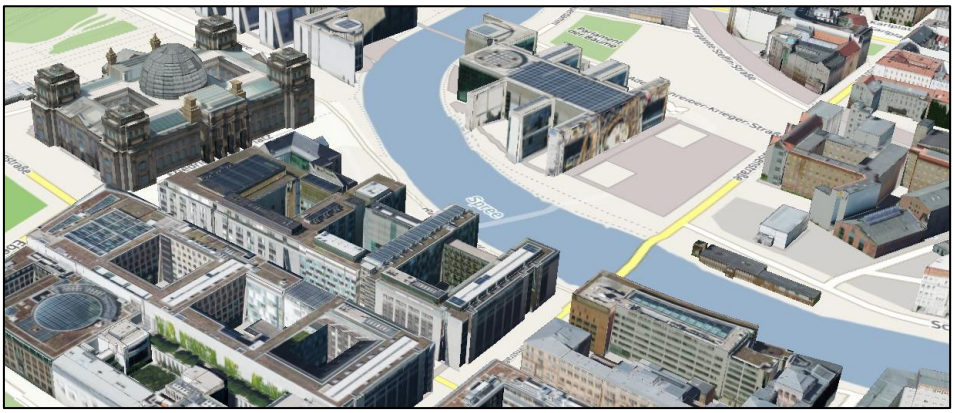

Fig. 2. Exemplary 3D data from Berlin (Image source: [8]).

to perform the further ray tracing steps, the city models were retrieved in *.3ds* format for easier use with standard 3D modelling software. The Spin 3D Mesh Converter [11] and Blender [12] were then utilized to convert the models to the open *.obj* file format and rescale the data correctly for import into Unity. In this preprocessing step the models of two different areas (booth about 5 km² in size) in Berlin were prepared for satellite visibility simulations as depicted in Fig. 3.

Ray Tracing Simulations

To generate realistic satellite visibility obstructions based on simulated UAV trajectories, the Unity 3D framework (see Fig. 4a) was used to perform raytracing simulations. While the raytracing algorithm itself is a built-in function in Unity, additional scripts had to be implemented and included to simulate trajectories through he 3D city landscapes and generate local maps for the sky visibility throughout the simulation.

In the suburban scenario we simulated the same drone trajectory in 2, 4 and 8 meters height above ground. For the urban canyon in the center of Berlin we simulate 2 and 8 meters. The plots in Figures 8 to 12 refer to these cases.

During the simulation, rays are cast all over the upper hemisphere, sampling every 0.5° along azimuth and elevation (i.e. 129600 samples per location along the simulated trajectory). Whenever the ray cast hits an obstacle (i.e. the path of the ray is blocked by a 3D object (building) from the city model), this part of the sky is considered obstructed. For each point along the simulated UAV trajectory, a local map is saved that contains the parts of the sky that are blocked seen from that point.

One exemplary result of such a raytracing step is given in Fig. 4b in form of a polar plot showing the upper hemisphere. The blue sections in the outer parts of the plot refer to parts of the sky obstructed by buildings. In the later simulations these sections are assumed as blocking the signals. In rare cases that might be over-conservative as sometimes thin (e.g. glass) structures of buildings could be included in the 3D models that do not necessarily block the satellite signals.

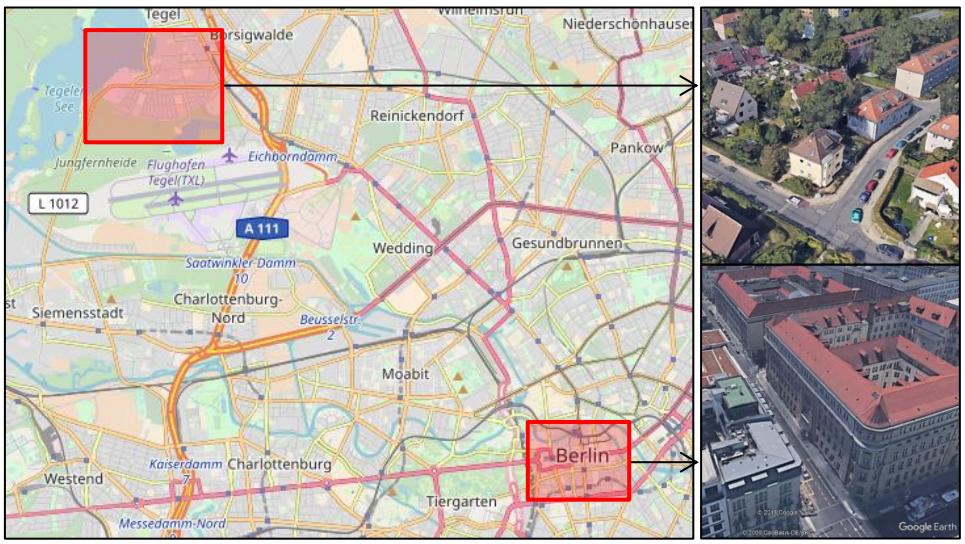

Fig. 3. Selected areas in Berlin for which data was downloaded and preprocessed. On the right an example image of the neighborhood is given (Source: openstreetmap.de, Google Earth)

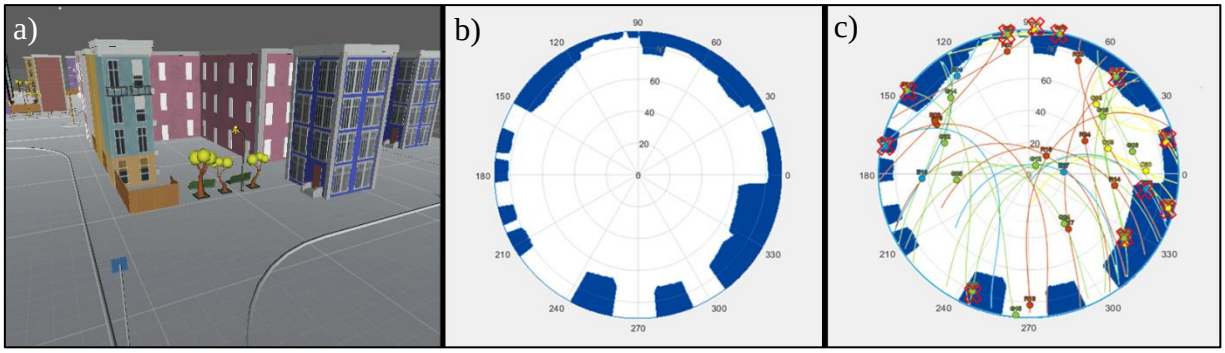

Fig. 4. Exemplary view within Unity Framework (a), resulting elevation mask (upper hemisphere) (b) and overlaid satellite orbits (c).

Constellation Visibility Simulations

In the next step towards assessing the performance of GNSS using local augmentation in urban scenarios, we use satellite almanac data from different constellations to simulate a large diversity of satellite distributions over the sky. While the GPS orbits repeat every day, i.e. from a certain location the satellites appear in the same azimuth and elevation again on the next day, this occurs for GLONASS and Galileo every 8 and 10 days respectively. We therefore choose to simulate orbits over a period of 10 days to cover for these periods. Nevertheless, as orbits change over time due to manoeuvring of the satellites and the constellations slowly shift among each other, that does not cover all the possible combinations (orbit configurations) but is considered representative enough for our purposes.

Assumed Airborne and Ground Residual Multipath and Noise models

In this work the focus is set on the satellite geometry implications when using satellite navigation in cities. Therefore we base our assumptions in terms of residual differential noise on signal level on values from literature complemented with own measurements ([7] [13]). In future work it is planned to use data collected within extensive flight testing with different drones to build models actually derived in urban scenarios.

Nevertheless, as in this study the comparisons are made between different urban scenarios and smoothing filter constants, the absolute navigation performance (in terms of achieved protection levels/position accuracy) is of lesser relevancy.

Airborne Nominal Navigation Performance

We perform the navigation performance evaluations and comparisons in this paper based on achieved nominal protection levels like they are used in GBAS or SBAS. Only a short summary will be given here. For detailed derivations and explanations we refer to literature like [14].

These protection levels define a bound on the position error with the required predefined probability. This probability is reflected in the protection level calculation (1) as fault-free-missed-detection multiplier (k_{ffmd}). For comparison purposes we will only refer to vertical protection levels (VPLs) as they are typically more stringent and also harder to achieve due to the satellite geometry (see [15]). Especially in urban environments this is true due to the regular blockage of low elevation satellite, important for precise lateral positioning.

The VPLs used later in the results are calculated as

$$VPL = k_{ffmd} \cdot \sqrt{\sum_{i=1}^{N} {s_{3,i}}^2 \cdot {\sigma_i}^2} \tag{1}$$

with ${\sigma_i}^2$as defined in (3) and $s_{3,i}$ referring to the i-th element in the third row of the pseudoinverse $\mathbf{S}$ of the weighted geometry matrix $\mathbf{G}$ containing all available satellites. N is the number of usable satellites, index i refers to satellite i.

$$S = (G^T W G)^{-1} \cdot G^T W \tag{2}$$

$\mathbf{G}$ is the satellite geometry matrix and $\mathbf{W}$ the diagonal matrix consisting of the residual differential noise terms for each used satellite. These noise terms are defined in (3):

$$\sigma = \sigma_{ground} + \sigma_{air} + \sigma_{iono} + \sigma_{tropo} \tag{3}$$

The assessment of the nominal airborne (H0) protection level performance is performed using the previously described intermediate results by combining the satellites locations over the period of 10 days with the local elevation masks (due to the obstacles along the trajectories) for flights of 20 minutes in length. The flight trajectory is about 7 km in lengths resulting in an average UAV speed of about 20 km/h or 5.6 m/s. To maximize the diversity in terms of local satellite geometry, these 20 minutes of flight are simulated 720 times covering the 10 days (see Fig. 5).

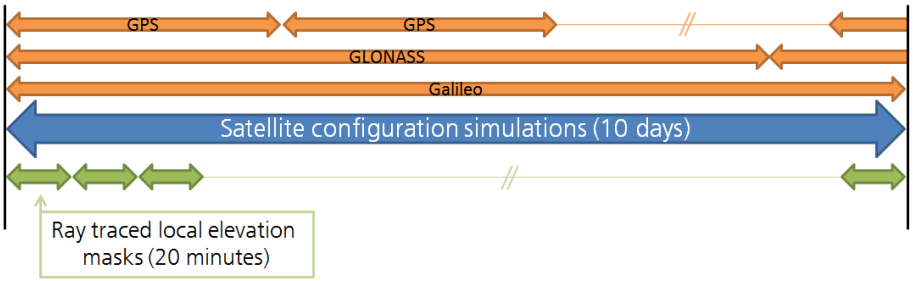

Fig. 5. A sketch of the simulation timeline (not to scale).
Within the 10 days of simulated constellations, 20 minutes of ray tracing results are used for 720 simulation runs.

RESULTS AND DISCUSSION

Residual Noise and Multipath

We start the results section by discussing the models for the residual noise and multipath used in the performance simulations. We base our simulations on the models for L1 frequencies shown in [13] that were derived from data collected with an actual UAV. The data provided here was resulting from a processing with 100 s smoothing time constant.

These values for σ_{air} were in a seconds step scaled to derive models for various smoothing time constants between 0 and 200 seconds. The scaling function is given in Fig. 6 and was derived from several hours of GNSS measurements taken by an antenna mounted on a moving car in an urban scenario with different receiver parameters to get an average estimate. The resulting σ_{air} models, showing the residual differential noise and multipath with respect to the satellite elevation are given in Fig. 7. We can see clearly, that quite short time constants reduce the noise significantly already. Smoothing for 10-15 seconds reduces the noise by about two thirds while doubling the time to 30 seconds gains hardly another 10 cm.

The used models for σ_{ground} were derived accordingly. In terms of σ_{iono} and σ_{tropo} standard GBAS models were applied as can be found with further explanation in [7] or [14].

Satellite Geometry

The second influencing parameter in terms of protection level performance as derived in (1) is the satellite geometry. This part is strongly influence by the local environment, as the loss or inclusion of a single satellite can potentially strongly influence the current geometry and therefore the projection of ranging errors into the position domain. In that sense, the satellite geometry is the part of the performance that is influenced differently by the different urban scenarios we consider in this work.

To give a first feeling of the influence of the suburban as well as the city-central scenario, we depict the number of visible and usable (i.e. converged smoothing filter) satellites for various cases in Fig. 8.

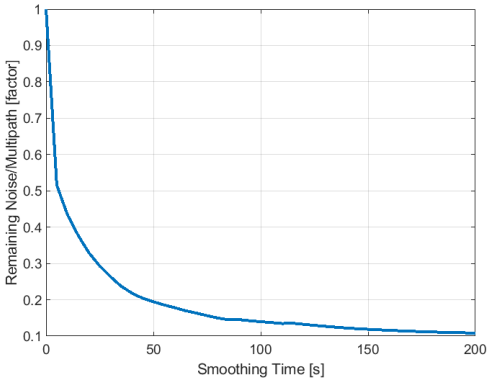

Fig. 6. Reduction of residual noise and multipath with growing smoothing time.

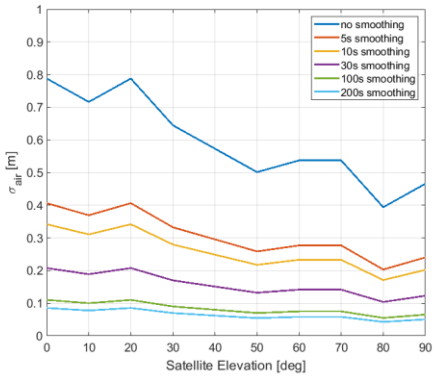

Fig. 7. Example of σ_{air} values over satellite elevation for selected smoothing times.

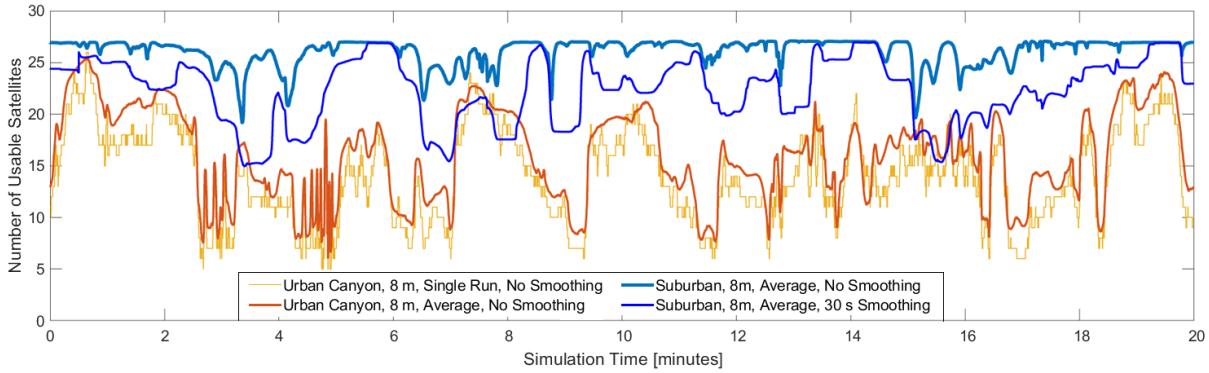

Fig. 8. Average number of usable satellites within 20 minutes of simulated drone trajectory.

A more statistical overview is given in Fig. 9. Here we show the average number of usable satellites with respect to the used smoothing filter convergence time for 5 scenarios. We can clearly see that in urban canyons already moderate smoothing times of about 30 seconds leave only about half of the visible satellites usable. Longer times will often lead to fewer available satellites than minimal required (3 + number of used constellations) for calculating a position.
In suburban areas with fewer high buildings, we see way more usable satellites, as one would expect. Also the decrease with smoothing time is less prominent.

Based on the usable satellite geometries we can in the next step compute the geometric dilution of precision (GDOP) in every simulated epoch along the drone trajectories. The DOP is a unitless factor describing how strong errors in the measurement domain (ranges) affect the positioning domain. Therefore, the smaller the (G)DOP value, the better.
In Fig. 10 we depict the behaviour of the DOP next to the average number of usable satellites to show the inverse relation. With increasing smoothing time constant fewer satellites are usable and thus the DOP increases. When we compare urban and suburban scenarios on that level, the differences are even more prominent. That can be explained by the distribution of visible satellites within an urban canyon. The remaining satellites are typically all very high elevation, creating an even weaker geometry than the number of satellites itself would suggest (see [15]).

Resulting VPL Performance
In a last step we now combine the residual noise considerations from the first section of the results with the geometric studies from right before and calculate achieved nominal protection levels for the same urban scenarios.
An average over all the 720 runs of 20 minutes is depicted in Fig. 11. As we expected, the protection levels in the urban canyon are significantly bigger. With increasing smoothing time they quickly reach dimensions that would not allow safe operations any longer. But more importantly in this study, we can find the minimum in terms of VPL and therefore

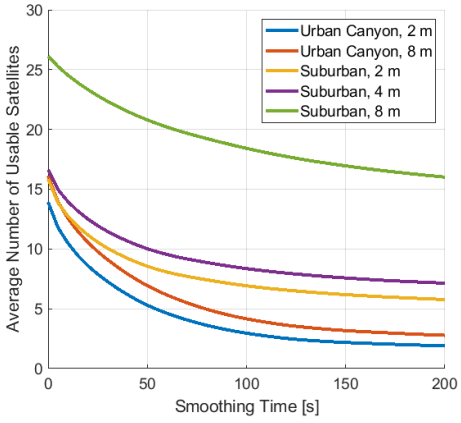

Fig. 9. Average number of usable satellites with respect to the smoothing time for different scenarios.

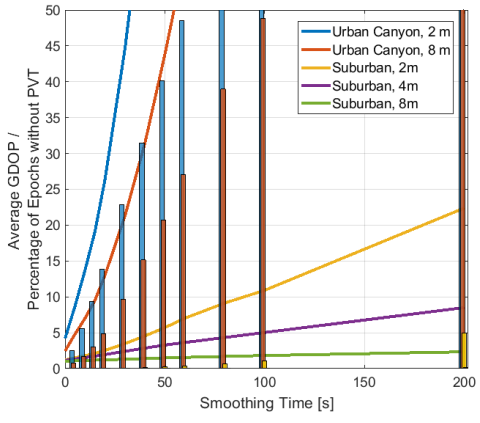

Fig. 10. Average achieved GDOP with respect to the smoothing time for different scenarios. The bars represent the percentage of epochs without enough usable satellites.

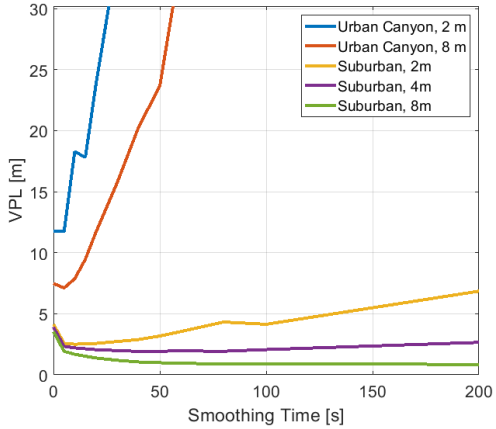

Fig. 11. Average achieved VPL with respect to smoothing time constant.

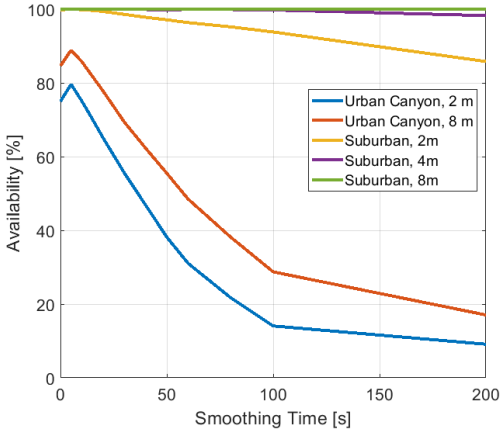

Fig. 12. Average achieved availability with respect to smoothing time constant.

optimal in terms of performance at only a few seconds in smoothing. Quickly after that point, the loss of satellites that are only visible for very short periods increases the VPL significantly.

In terms of suburban scenarios we find a totally different situation. While the most demanding situation with the drone only 2 meters above ground level shows a similar minimum at 5-10 seconds smoothing, the two other scenarios show best performance at 50 and 200 seconds respectively. While 4 meters above ground the effect of losing satellites is still visible, leading to slowly increasing VPLs towards very long smoothing times, this is not true anymore for 8 meters.

In Fig. 12 we provide availability (i.e. fraction of time/epochs in which the protection level is below in this case 10 m) as another metric to assess the performance. In general we find the results from Fig. 11 confirmed in the plot. While the performance in the urban canyon is poor in most of the configurations, in suburban areas good availability can be achieved mostly. What is only visible in the availability plot is that with increasing smoothing time, more and more unavailable epochs occur also in suburban areas. While the protection levels increase only moderately in case of the 2 m suburban scenario, the availability drops to only about 85%.

CONCLUSIONS AND FUTURE WORK

Conclusions

In this work we presented a simulation environment for satellite visibility and GNSS navigation performance based on 3D city models. Using 3D models from Berlin we simulated different triple constellation, single frequency L1 GNSS scenarios and evaluated the influence of different smoothing filter convergence times on the navigation performance.

We separately evaluated the influence of carrier smoothing with smoothing time constants from 0 to 200 s on residual noise and multipath as well as on the satellites geometries. In a last step both parts were combined to assess resulting protections levels in the different urban scenarios and find optimal convergence times accordingly.

Large differences could be seen here between urban (canyons) and suburban scenarios. In suburban areas without densely built-up areas the positive effect of longer smoothing is dominant, especially when flying 4 m or more about ground. In urban canyons performance is largely driven by the number of usable satellites, leading to best performance and availability for very short smoothing times of 0 to 10 seconds.

Future Work and Open Points

The herein presented framework is just a first step towards more complex scenarios. Simulations of realistic drone operations (take-off, mission, landing) throughout a city are planned in a next step. These can then also be compared to real measurement taken along the same trajectories. The speed of the drone was fixed at 20km/h in the current simulations. This would be another parameter potentially benefitting shorter smoothing times constants in case of increased drone speed.

The framework shall also be extended to L5 frequency which promises better navigation performance especially in multipath-heavy environments but is also better suited for short smoothing time constants due to lower initial noise levels. Multipath in general is also not considered in the current simulations. Future work shall show whether the 3D-models are accurate enough already to give indications at least in terms of severity of multipath in a certain area.

Finally, also the implications on airborne integrity monitoring in case of shorter carrier smoothing times have to be studied.

REFERENCES

[1] S. Pullen, P. Enge and J. Lee, "Local-Area Differential GNSS Architectures Optimized to Support Unmanned Aerial Vehicles (UAVs)," 2013.

[2] S. Pullen, "Managing Separation of Unmanned Aerial Vehicles Using High-Integrity GNSS Navigation," in *EIWAC 2013*, Tokyo, Japan, 2013.

[3] D. Kim, J. Lee, M. Kim, J. Lee and S. Pullen, "High-Integrity and Low-Cost Local-Area Differential GNSS Prototype for UAV Applications," in *Proceedings of the 30th International Technical Meeting of The Satellite Division of the Institute of Navigation (ION GNSS+ 2017)*, 2017.

[4] M. Kim, D.-K. Lee and E. Bang, "Conceptual Study of Mobile Differential GNSS Architecture Utilizing UAV Networks," in *Proceedings of the ION 2015 Pacific PNT Meeting*, 2015.

[5] J. Lee, M. Kim, J. Lee and S. Pullen, "Integrity assurance of Kalman-filter based GNSS/IMU integrated systems against IMU faults for UAV applications," in *Proceedings of the 31st International Technical Meeting of The Satellite Division of the Institute of Navigation (ION GNSS+ 2018)*, Miami, Florida, 2018.

[6] R. Hatch, "The Synergism of GPS code and carrier measurements," *International Geodetic Symposium on Satellite Doppler Positioning, 3rd, Las Cruces, NM, February 8-12, 1982, Proceedings,* vol. 2, pp. 1213-1231, 1982.

[7] D. Gerbeth, M.-S. Circiu, M. Caamano and F. Michael , "Nominal Performance of Future Dual Frequency Dual Constellation GBAS," *International Journal of Aerospace Engineering*, pp. 1-20, 2016.

[8] Berlin Partner für Wirtschaft und Technologie GmbH, "Berlin 3D - Downloadportal," virtualcitySYSTEMS GmbH, [Online]. Available: https://www.businesslocationcenter.de/berlin3d-downloadportal. [Accessed 28 09 2018].

[9] Special Interest Group 3D, "CityGML Homepage," 2018. [Online]. Available: https://www.citygml.org/.

[10] Unity Technologies, "Unity," 2018. [Online]. Available: https://unity3d.com/de.

[11] NCH Software, "Spin 3D Modellkonverter," [Online]. Available: www.nchsoftware.com/3dconverter/de/.

[12] Blender Foundation, "Blender," 1998-2018. [Online]. Available: www.blender.org/.

[13] M.-S. Circiu, M. Felux, B. Belabbas, M. Meurer, J. Lee, M. Kim and S. Pullen, "Evaluation of GPS L5, Galileo E1 and Galileo E5a Performance in Flight Trials for Multi Frequency Multi Constellation GBAS," in *Proceedings of ION GNSS+ 2015*, 2015.

[14] Radio Technical Commission for Aeronautics, "RTCA DO-253D. Minimum Operational Performance Standards for GPS Local Area Augmentation System Airborne," 2017.

[15] D. Gerbeth, M. Felux, M.-S. Circiu and M. Caamano, "Optimized Selection of Satellite Subsets for a Multi-Constellation GBAS," in *Proceedings of the 2016 International Technical Meeting of The Institute of Navigation*, Monterey, CA, USA, 2016.